CrossMark

# Tunable Slow Light in Graphene Metamaterial in a Broad Terahertz Range

S. Izadshenas[1] · A. Zakery[1] · Z. Vafapour[1]

**Abstract** A graphene-based metamaterial with tunable electromagnetically induced transparency is numerically studied in this paper. The proposed structure consists of a graphene layer composed of H shape between two cut wires, by breaking symmetry can control EIT-like effects and by increasing the asymmetry in the structure has strong coupling between elements. It is important that the peak frequency of transmission window can be dynamically controlled over a broad frequency range by varying the chemical potential of graphene layer. The results show that high refractive index sensitivity and figure of merit can be achieved in asymmetrical structures which is good for sensing applications. We calculated the group delay and the results show we can control the group velocity by varying the S parameter in asymmetrical structure. The characteristics of our system indicate important potential applications in integrated optical circuits such as optical storage, ultrafast plasmonic switches, high performance filters, and slow-light devices.

**Keywords** Electromagnetically induced transparency · Graphene · Slow light · Refractive index sensing

## Introduction

Electromagnetically induced transparency (EIT) is a quantum effect that enhances light transmission over a narrow spectral region [1–3]. Modification of the dispersive properties of the medium along with this enhancement of transmission leads to a slowing down of the incident light [4–7]. EIT has many applications such as ultraslow light propagation [4], light storage [6, 8], dissipation-free light transmission, and nonlinear optics.

Recently, attention has been paid to the fact that EIT-like effects in classical systems such as micro resonators [9], electric circuits [10], and metallic structures [11] are observed. Theoretical predictions of plasmon-induced transparency have been supported by experimentally observed Fano resonances within an absorption band at optical frequencies [12, 13]. Because of the broad linewidth of these resonance applications such as slowing down light, which requires an abrupt change in dispersion over a narrow spectral range, is not possible [14].

By controlling the resonant elements of the metamaterial structures, it is possible to dynamically control their optical response and hence expand the range of their applications. By reconstructing the geometries of the metamaterial structure or modifying the supporting substrate, it is possible to achieve tuning of the transparency window. Integrating metamaterials with materials with tunable permittivity, such as graphene, has been recently investigated for plasmonic devices [15]. Graphene is a very good candidate for designing and fabrication of tunable devices because its conductivity can be controlled by tuning its Fermi level energy from $-1$ to $1$ eV by doping [16] or electrostatic gating [17]. Graphene can strongly interact with light over a wide frequency range and it is suited for the mid-IR frequency range because it has strong plasmonic response as well as having a small loss.

Up to now, the research of EIT in metamaterials has focused on two main approaches: the bright-bright mode coupling [18] and the bright-dark coupling [19, 20]. Becker

✉ A. Zakery
  zakeri@susc.ac.ir

[1] Department of Physics, College of Science, Shiraz University, Shiraz, 71946-84795, Iran
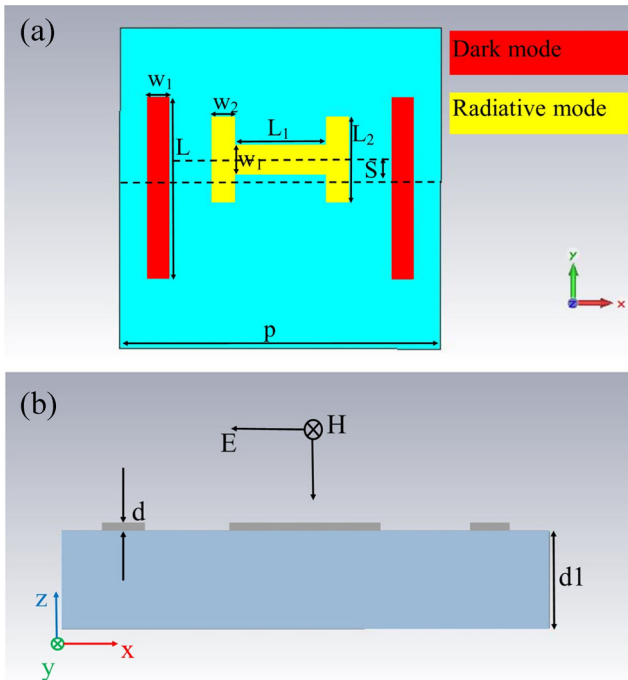
**Fig. 1** **a** Schematic of the metamaterial design. **b** Cross-section view and the incident light polarization. The geometric parameters are $p = 500$ nm, $w_1 = 30$ nm, $L = 280$ nm, $w_1 = w_2 = 30$ nm, $L_1 = 150$ nm, $L_2 = 130$ nm

et al. calculated sensitivity of gold nanorods from plasmon resonance of metal nanoparticles shifts upon refractive index changes [21]. Ding et al. demonstrated a graphene ribbon array and square closed ring resonator separated by a dielectric substrate that by decreasing the thickness
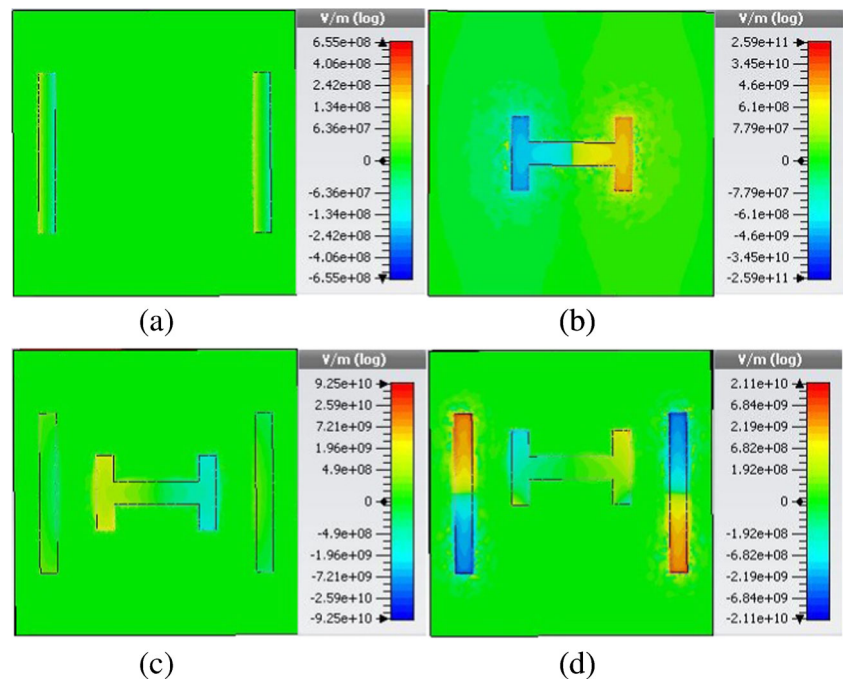
of substrate controls EIT effects [22]. Hu et al. achieved high sensitivity by using symmetry breaking [23]. Huang et al. used plasmonic-induced transparency based on stub waveguide with nanodisk resonator and achieved the group index over 88 [24]. Liu et al. demonstrated multispectral sharp plasmon-induced transparency in a hybrid waveguide plasmon system that has a high figure of merit [25].

This paper is organized as follows. In the "Proposed Design" section, we explain the geometrical parameters in the proposed metamaterial. In the "Interaction of Incident Light with Nanostructures" section, we investigate the coupling between incident light and plasmonic modes (dark and radiative plasmonic modes) shown in Fig. 3. Moreover, we illustrate the electric field distribution for better understanding of underlying physics. In the "Asymmetrical Structure and EIT-Like effects" section, we perform a detailed study of the EIT effect in suggested structure with broken symmetry. Furthermore, we illustrate the magnetic field distribution for better understanding of underlying physics. In the "Influence of Refractive Index on EIT-Like Effects" section, we investigate the influences of the refractive index on the observed EIT phenomenon. We investigate the sensitivity of the structure. In the "Influence of Chemical Potential on EIT-Like effects" and "Influence of Asymmetry on Sensitivity" sections, we show the highest Q factor in the proposed metamaterial. Finally, in the "Group Delay" section, we analyze the group delay. A dramatic reduction factor for the group velocity has also been achieved via EIT in this structure, which is the highest value for the reduction factor reported to date in lossy plasmonic metals with using graphene in the proposed metamaterial. Main results are summarized in the "Conclusion" section.

**Fig. 2** Electric field near the nanostructure at transmittance peak
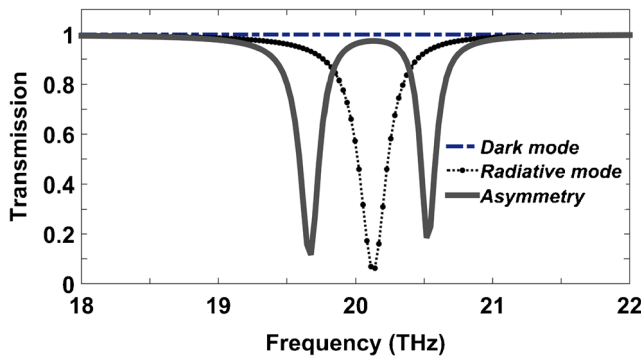
**Fig. 3** Transmission spectra of the dark, radiative mode in symmetric and asymmetrical structure

## Proposed Design

The unit cell of the graphene-based EIT metamaterial proposed here is shown in Fig. 1a [26]. The graphene layer and the substrate are illustrated in gray and blue, respectively. This nanostructure is composed of three graphene bars printed on a substrate. The dielectric constant of the substrate is 2.4025. Figure 1a displays the top view of a unit cell of the structure; the two parallel bars which are shown in red are the dark elements and the H-shape bar shown in yellow is the bright element. The unit cell with dimension of $p \times p$ is composed of a graphene H shape and two graphene cut wires (CW) and is attached to a substrate and the substrate is in the x-y plane. The H shape contains two identical arms with length of $L_2$ and a width of $w_2$ and a base with a

length of $L_1$ and a width of $w_1$. The CWs have a length of $L$ and width of $w_1$. The H shape and CW elements are symmetrically aligned and separated from each other by $S$. the designed devices are investigated in the infrared frequency range at around $1 \sim 30$ THz.

All the designed graphene-based tunable metamaterial structures with EIT-like transparency windows are numerically studied by commercial package CST Microwave Studio. The optical conductivity of graphene consists of the intraband and interband contributions and is related to the chemical potential [27], through

$$
\sigma = \frac{j}{\omega + 1/\tau} \frac{e^2 2 k_B T}{\pi \hbar^2} \ln \left[ 2 \cosh \frac{\mu_c}{2 k_B T} \right]
$$
$$
+ \frac{e^2}{4\hbar} \left[ G(\frac{\hbar \omega}{2}) + j \frac{4\hbar \omega}{\pi} \int_0^\infty \frac{G(\zeta) - G(\frac{\hbar \omega}{2})}{(\hbar \omega)^2 - 4\zeta^2} d\zeta \right] \quad (1)
$$

where

$$
G(\zeta) = \frac{\sinh (\zeta / k_B T)}{[\cosh (\mu_c / k_B T) + \cosh (\zeta / k_B T)]} \quad (2)
$$

$e$, $k_B$, and $\hbar$ are the charge of electron, the Boltzmann constant, and the reduced Planck constant, respectively. We assume an electron scattering life time $\tau = 3$ ps and a room temperature of $T = 300$ K in Eq. 1. We can see from Eq. 1 that changing the chemical potential $\mu_c$ enables the control of the propagation characteristics of the graphene plasmons. The dielectric constant of graphene can be calculated through $\epsilon = 1 + \frac{j\sigma}{\epsilon_0 \omega d}$, where $d$ is the thickness of graphene layer in modeling and simulation. We adopt $d = 1$ nm throughout our simulations.

**Fig. 4** Calculated **a** transmission, **b** reflectance, and **c** absorption in asymmetrical and symmetrical cases
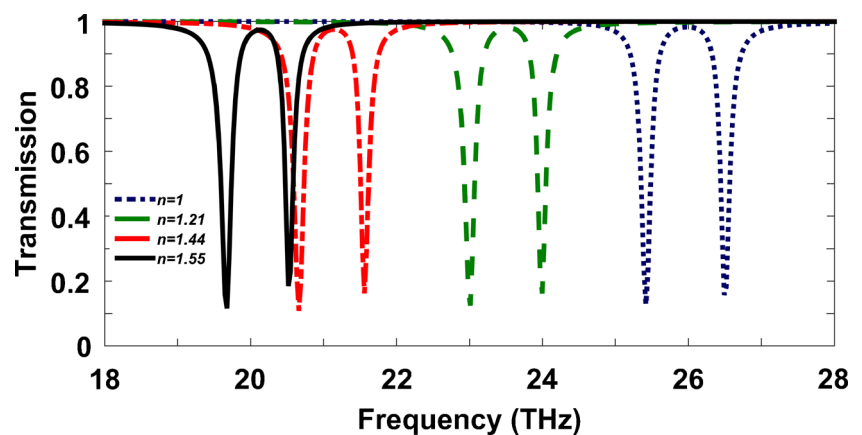


(a)



(b)



(c)

(a)



(b)
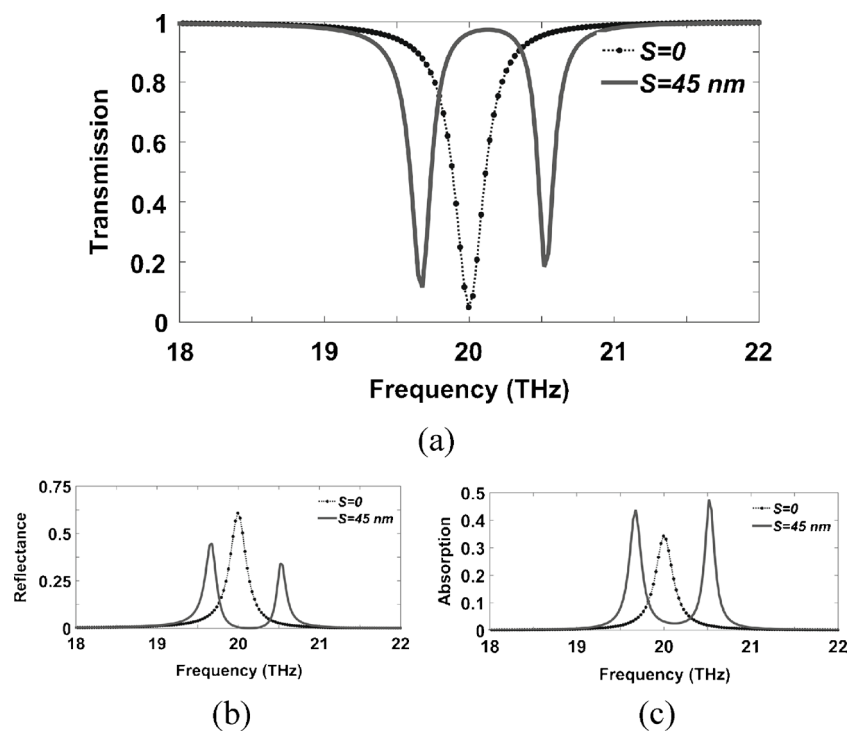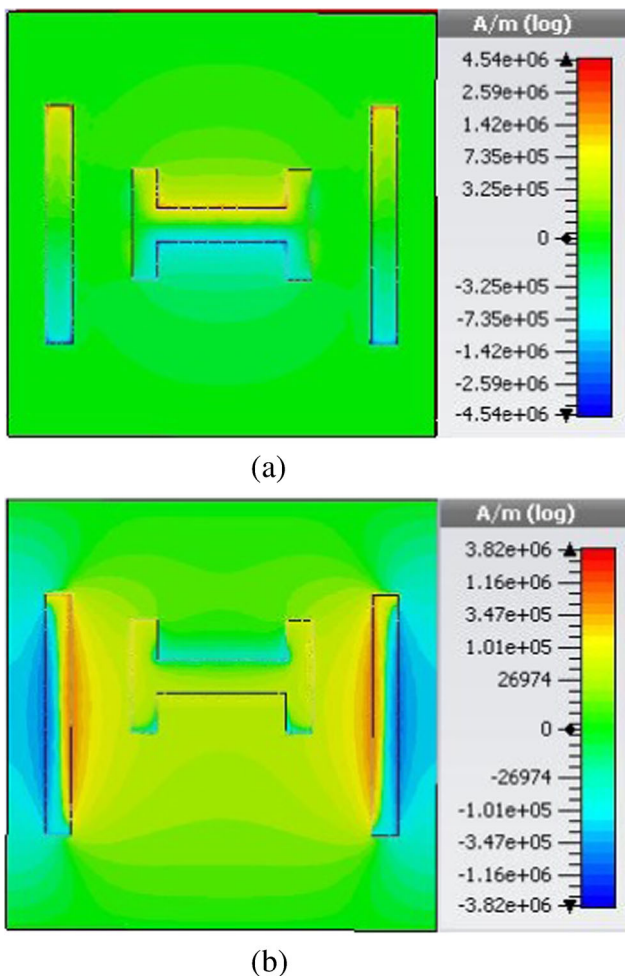
**Fig. 5** Magnetic field near the nanostructure at transmittance peak

## Interaction of Incident Light with the Nanostructures

In this section, we investigate the interaction of light with the nanostructures. This interaction is investigated for cases

of bright element only, dark elements only, bright and dark elements in the symmetric case, and bright and dark elements in the asymmetric case. As shown in Fig. 2a, the incident light has no interaction with the dark element and hence no resonance is observed for this interaction; therefore, this element is called a dark mode. We now consider the interaction of the incident light with the H-shape bar. As shown in Fig. 2b, the interaction of the incident light with this element induces a dipole in this bar and oscillation of this dipole causes a resonance for this element which is shown in Fig. 3. By inserting the H-shape bar between the two parallel bars and hence keeping the symmetry of the nanostructure ($S = 0$), the interaction of the incident light with this structure is studied. As shown in Fig. 2c, a strong electric interaction is induced in bright element but because the electric fields are equal in opposite sides of the H bar element, they cancel each other out and only a single resonance is observed. If we now break the symmetry and as it is observed in Fig. 2d, electric fields in opposite sides of the H bar element are no longer equal and this leads to the creation of a quadrupole in the two parallel bars. As a result of the destructive coupling of this quadrupole with the dipole, an EIT phenomenon is observed. Hence, EIT phenomenon is due to creation of the quadrupole in the two parallel bars and a destructive interaction of this quadrupole with the dipole.

## Asymmetrical Structure and EIT-Like Effects

As it is mentioned before, EIT is due to a destructive interaction in the system. In this part, we investigate the effect of asymmetry and interaction of electric fields in the structure. First, we consider the symmetric structure ($S = 0$   nm) that was not predicted to lead to the EIT. Since many parametric studies of EIT systems have been reported [28], we will not discuss all the optimization parameters here but instead focus on the new regimes of the EIT enabled in this

**Fig. 6** Calculated transmittance spectra of the proposed metamaterial structure in air and immersed in $n = 1.21$, $n = 1.44$, $n = 1.55$, respectively

**Fig. 7** Sensing characteristics of EIT-based sensor. **a** Sensitivity of the proposed sensor. **b** FOM of the proposed sensor. **c** Relation between the transparency peak shift $\Delta\lambda$ and the refractive index variation $\Delta n$ of the surrounding medium



(a)



(b)



(c)
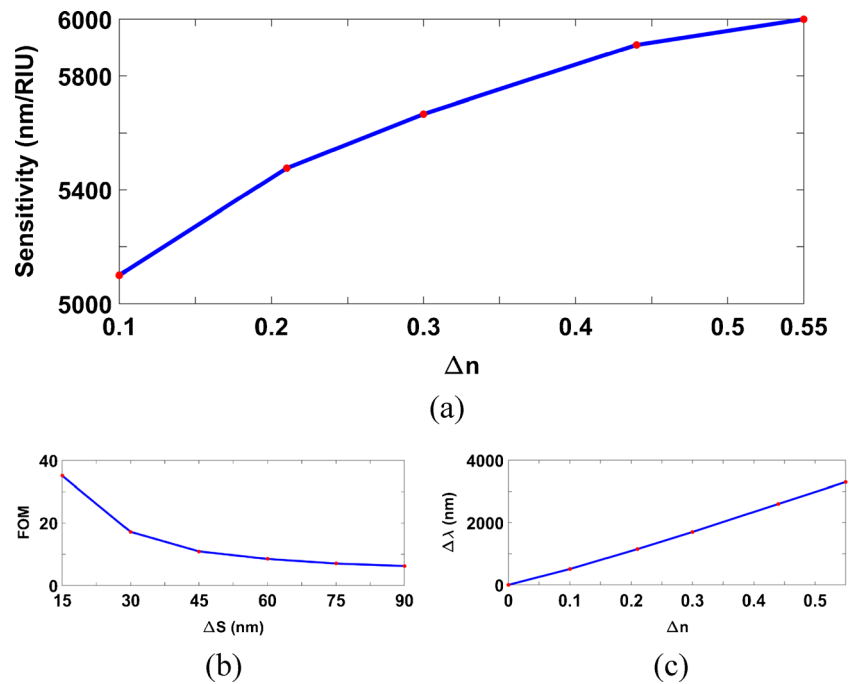
structure. If the structure is symmetric, a single resonance is observed which is shown in Fig. 4a which is due to the existence of the dipole in the H-shape bar shown in Fig. 5a. By breaking the symmetry in the structure, a quadrupole is induced in the two parallel bars which is shown in Fig. 5b, as a result of destructive interaction between them leading to EIT shown in Fig. 4a. As is shown in Fig. 4a, by increasing

the S parameter the transmission increases and absorption and reflection decrease at the resonance frequency which are shown in Fig. 4b, c, respectively. The reason for the increase in transmission and decrease in reflectance is the stronger coupling between the dark and bright elements. For plotting the absorption spectrum, we used the relation $A = 1 - R - T$.

**Fig. 8** **a** Transmission, **b** reflectance, and **c** absorption spectra of the metamaterial EIT for various chemical potentials
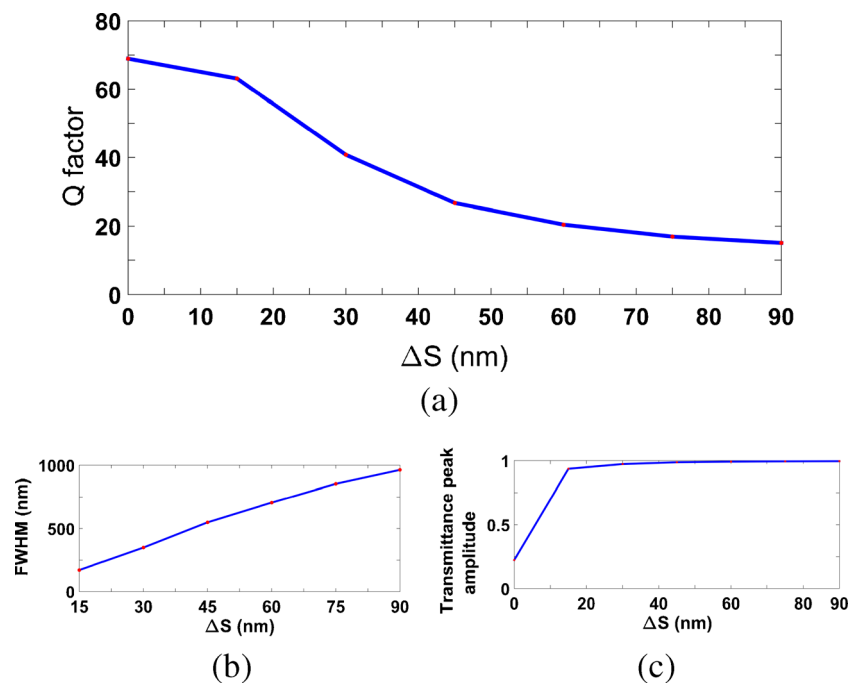


(a)



(b)



(c)
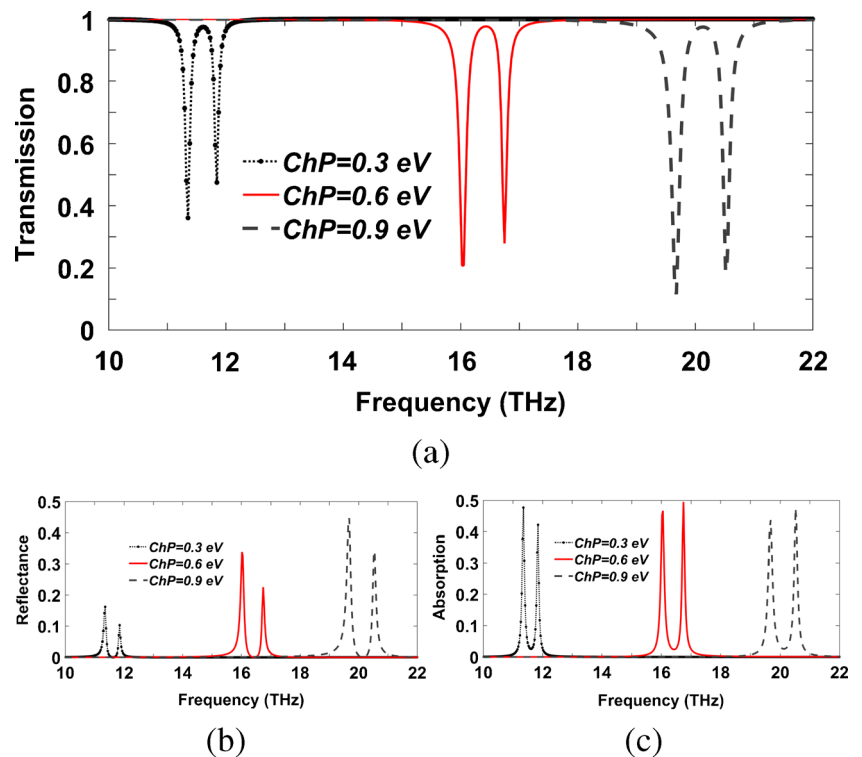
## Influence of Refractive Index on EIT-Like Effects

One of the characteristics of metamaterials is their use for the design of refractive index-based sensors in which by a change of the refractive index of the surrounding medium the resonance frequency of the sensor changes [29]. In these materials, it is possible to investigate the sensitivity of the sensor to refractive index changes between 1 to 1.55 as well as their figure of merit (FOM). Figure 6 shows transmittance versus the refractive index and as is shown the resonance peak has a shift towards lower frequencies. For example, by considering the refractive index of the substrate to be 1, the resonance peak occurs at a frequency of 27.64 THz. By changing the refractive index to a value of 1.21 and 1.55, the resonance peak shifts to 23.2 and 20.38 THz, respectively. This is due to the fact that the resonance peak shifts to lower frequencies for higher refractive index of the surrounding medium [29]. For investigating the sensitivity, we define it as the amount of frequency shift over the refractive index change (RIU). As it is shown in Fig. 7a, the sensitivity versus the refractive index change and the sensitivity maximum is equal to 6000 nm/RIU. Since EIT occurs in an asymmetric structure and this depends on the $S$ value, we use the definition of FOM and plot it against the $S$ parameter. This is shown in Fig. 6b and also in Fig. 7c by increasing the refractive index change the amount of frequency change increases. As it is seen, a value of 12.5 is obtained for a value of $S = 45$ nm. This value is much higher than for the sensors based on resonance surface plasmons using nanobars having a value of FOM = 5.3 [30] and nanoparticles having FOM = 1.3 [31].

## Influence of Chemical Potential on EIT-Like Effects

One of the interesting features of graphene is the tunability of its dielectric constant which depends on four parameters such as frequency, temperature, chemical potential, and electron scattering life time. Chemical potential is of course a more important parameter [32–34]. In fact, by changing the chemical potential, the electron density in graphene changes which leads to a frequency shift of the spectral response [35]. Therefore, by controlling the dielectric constant of the graphene, it is possible to obtain a tunable frequency range for the occ urrence of EIT using a graphene layer in the nanostructure. As is shown in Fig. 8a, the transmittance spectrum is plotted for an asymmetric structure and a frequency shift from 11.6 to 20.14 THz is obtained by changing the chemical potential from 0.3 to 0.9 eV. This tunability of the frequency change has many applications such as in switches and modulators.

## Influence of Asymmetry on Sensitivity

In this section, we investigate the effect of change in the symmetry of the structure on spectral response of the system. Fig. 9a shows the Q factor versus the $S$ parameter. As is shown, the Q factor decreases by increasing the S parameter. This is due to an increase of the full width half maximum (FWHM) with an increase of the $S$ parameter which is shown in Fig. 9b. It is also shown that by an increase of the $S$ parameter, the peak height increases which is shown in

**Fig. 9** Influence of structural asymmetry on properties of transparency window. **a** Q-factor. **b** FWHM. **c** Amplitude of the transmittance peak



(a)



(b)



(c)

Fig. 9c. For calculating the Q factor, we have used the definition of frequency over the full width half maximum. For example, the value of Q factor for $S = 15$ nm is 63.135 and the peak transmittance is 0.87 while the Q factor is 15.01 for $S = 90$ nm and the peak transmittance is 0.99. Fig. 9a, c shows that an inverse relation exists between the Q factor and the transmittance peak.

## Group Delay

One of the results of the EIT effect is slowing down of the light velocity. This has an important role in optical information. In fact, the positive and negative value of the group velocity is related to slowness of the light [4, 36]. In this part, we investigate the effect of EIT in a structure based on graphene on the speed of light. We can define the group velocity as follows:

$$V_g = \frac{C}{n_g} = \frac{L}{\tau_g} \tag{3}$$

where $L$ is the thickness of the medium through which light passes, $C$ is the light velocity, and $n_g$ and $\tau_g$ are the group index and group delay, respectively. Figure 10a shows the change in group delay for three different chemical potentials
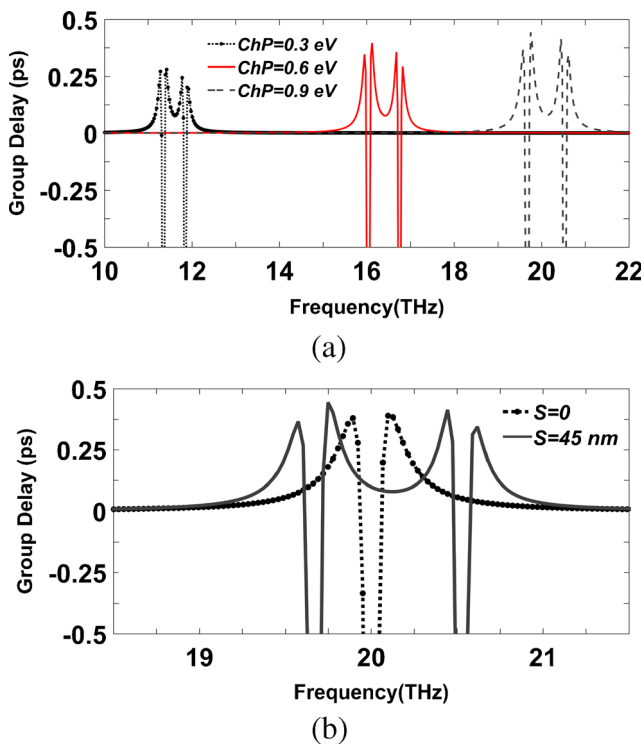
[9, 37]. An investigation of the group delay in graphene for symmetric and asymmetric structures is shown in Fig. 10b. As we predicted, the EIT effect could lead to a decrease of the group velocity in the structure. As this diagram shows, wherever the EIT effects are observed in this structure, the group velocity has changed by a factor of 300. Therefore, the group velocity decreases drastically in the frequency range where the EIT effect occurs.

## Conclusion

In conclusion, we show that using a graphene layer composed of H shape between two cut wires can lead to EIT-like effects by asymmetrical structures or we can say coupling between dark-bright modes created EIT-like effects. We show that we have a structure based on refractive index sensing that have high sensitivity about 6000 nm/RIU with good applications for biochemicals. An important feature is that by varying the chemical potential, we can tune the transparency peak over a broad frequency range. The results showed that by increasing the $S$ parameter, the Q factor decreased and the transmittance peak amplitude increased. The high transmittance peak amplitude is over 99.5%. We calculated the group delay and showed that by varying the $S$ parameter, we can control the group velocity and we can have slow light about an order of 300 that is valuable for slow light applications.



**Fig. 10** Group delay spectra of the graphene EIT structure under normal incidence at different chemical potentials

## References

1. Boller KJ, Imamolu A, Harris SE (1991) Observation of electromagnetically induced transparency. Phys Rev Lett 66(20):2593
2. Fleischhauer M, Imamoglu A, Marangos JP (2005) Electromagnetically induced transparency: optics in coherent media. Rev Mod Phys 77(2):633
3. Marangos JP (1998) Electromagnetically induced transparency. J Mod Opt 45(3):471–503
4. Hau LV, Harris SE, Dutton Z, Behroozi CH (1999) Light speed reduction to 17 metres per second in an ultracold atomic gas. Nature 397(6720):594–598
5. Shvets G, Wurtele JS (2002) Transparency of magnetized plasma at the cyclotron frequency. Phys Rev Lett 89(11):115003
6. Liu C, Dutton Z, Behroozi CH, Hau LV (2001) Observation of coherent optical information storage in an atomic medium using halted light pulses. Nature 409(6819):490–493
7. Lukin MD (2001) Controlling photons using electromagnetically induced transparency. Nature 413(6853):273–276
8. Phillips DF, Fleischhauer A, Mair A, Walsworth RL, Lukin MD (2001) Storage of light in atomic vapor. Phys Rev Lett 86(5):783
9. Xu Q, Sandhu S, Povinelli ML, Shakya J, Fan S, Lipson M (2006) Experimental realization of an on-chip all-optical analogue to electromagnetically induced transparency. Phys Rev Lett 96(12):123901
10. Alzar CG, Martinez MAG, Nussenzveig P (2002) Classical analog of electromagnetically induced transparency. Am J Phys 70(1):37–41

11. Papasimakis N, Fedotov VA, Zheludev NI, Prosvirnin SL (2008) Metamaterial analog of electromagnetically induced transparency. Phys Rev Lett 101(25):253903

12. Zhang S, Genov DA, Wang Y, Liu M, Zhang X (2008) Plasmon-induced transparency in metamaterials. Phys Rev Lett 101(4):047401

13. Verellen N, Sonnefraud Y, Sobhani H, Hao F, Moshchalkov VV, Dorpe PV, Maier SA (2009) Fano resonances in individual coherent plasmonic nanocavities. Nano Lett 9(4):1663–1667

14. Hao F, Sonnefraud Y, Dorpe PV, Maier SA, Halas NJ, Nordlander P (2008) Symmetry breaking in plasmonic nanocavities: subradiant LSPR sensing and a tunable Fano resonance. Nano Lett 8(11):3983–3988

15. Bao Q, Loh KP (2012) Graphene photonics, plasmonics, and broadband optoelectronic devices. ACS Nano 6(5):3677–3694

16. Chuang FT, Chen PY, Cheng TC, Chien CH, Li BJ (2007) Improved field emission properties of thiolated multi-wall carbon nanotubes on a flexible carbon cloth substrate. Nanotechnology 18(39):395702

17. Hanson GW (2008) Dyadic Green's functions for an anisotropic, non-local model of biased graphene. IEEE Trans Antennas Propag 56(3):747–757

18. Jin XR, Park J, Zheng H, Lee S, Lee Y, Rhee JY, Jang WH (2011) Highly-dispersive transparency at optical frequencies in planar metamaterials based on two-bright-mode coupling. Opt Express 19(22):21652–21657

19. Vafapour Z, Zakery A (2016) New approach of plasmonically induced reflectance in a planar metamaterial for plasmonic sensing applications. Plasmonics 11(2):609–618

20. Liu N, Langguth L, Weiss T, Kstel J, Fleischhauer M, Pfau T, Giessen H (2009) Plasmonic analogue of electromagnetically induced transparency at the Drude damping limit. Nat Mater 8(9):758–762

21. Becker J, Trgler A, Jakab A, Hohenester U, Snnichsen C (2010) The optimal aspect ratio of gold nanorods for plasmonic biosensing. Plasmonics 5(2):161–167

22. Ding J, Arigong B, Ren H, Shao J, Zhou M, Lin Y, Zhang H (2015) Dynamically tunable fano metamaterials through the coupling of graphene grating and square closed ring resonator. Plasmonics 10(6):1833–1839

23. Hu X, Huang Y, Yuan S, Liu Y, Jiao Z, Wang Y, Xia J (2015) A high sensitivity plasmonic structure by using electric and magnetic plasmon modes. Plasmonics 10(6):1817–1824

24. Huang B, Meng H, Wang Q, Wang H, Zhang X, Yu W, Wang F (2016) Plasmonic-induced transparency and slow-light effect based on stub waveguide with nanodisk resonator. Plasmonics 11(2):543–550

25. Liu J, Xu B, Zhang J, Song G (2013) Double plasmon-induced transparency in hybrid waveguide-plasmon system and its application for localized plasmon resonance sensing with high figure of merit. Plasmonics 8(2):995–1001

26. Vafapour Z, Zakery A (2015) New regime of plasmonically induced transparency. Plasmonics 10(6):1809–1815

27. Falkovsky LA (2008) Optical properties of graphene. J Phys Conf Ser 129(1):012004. IOP Publishing

28. Vafapour Z, Alaei H (2016) Achieving a high Q-factor and tunable slow-light via classical electromagnetically induced transparency (Cl-EIT) in metamaterials. Plasmonics. doi:10.1007/s11468-016-0288-0

29. Meng FY, Wu Q, Erni D, Wu K, Lee JC (2012) Polarization-independent metamaterial analog of electromagnetically induced transparency for a refractive-index-based sensor. IEEE Trans Microw Theory Tech 60(10):3013–3022

30. Liu N, Weiss T, Mesch M, Langguth L, Eigenthaler U, Hirscher M, Giessen H (2009) Planar metamaterial analogue of electromagnetically induced transparency for plasmonic sensing. Nano Lett 10(4):1103–1107

31. Wang H, Brandl DW, Le F, Nordlander P, Halas NJ (2006) Nanorice: a hybrid plasmonic nanostructure. Nano Lett 6(4):827–832

32. Wunsch B, Stauber T, Sols F, Guinea F (2006) Dynamical polarization of graphene at finite doping. New J Phys 8(12):318

33. Hwang EH, Sarma SD (2007) Dielectric function, screening, and plasmons in two-dimensional graphene. Phys Rev B 75(20):205418

34. Jablan M, Buljan H, Soljai M (2009) Plasmonics in graphene at infrared frequencies. Phys Rev B 80(24):245435

35. Wang F, Zhang Y, Tian C, Girit C, Zettl A, Crommie M, Shen YR (2008) Gate-variable optical transitions in graphene. Science 320(5873):206–209

36. Schnorrberger U, Thompson JD, Trotzky S, Pugatch R, Davidson N, Kuhr S, Bloch I (2009) Electromagnetically induced transparency and light storage in an atomic Mott insulator. Phys Rev Lett 103(3):033003

37. Yanik MF, Suh W, Wang Z, Fan S (2004) Stopping light in a waveguide with an all-optical analog of electromagnetically induced transparency. Phys Rev Lett 93(23):233903